Electronic Supporting Information for

Catalytic Reduction of Dioxygen to Water with a Monomeric Manganese Complex at Room Temperature

Ryan L. Shook,† Sonja M. Peterson,† John Greaves,† Curtis Moore,‡ Arnold L. Rheingold‡ and A.S. Borovik*†

Department of Chemistry, University of California-Irvine, 1102 Natural Science II, Irvine, CA 92697-2025 and the Department of Chemistry and Biochemistry, University of California-San Diego, San Diego, 92093-0332

Email: aborovik@uci.edu

Contents

Table S1. Results from Reactions of $[Mn^{II}H_2bupa]^-$ with DPH and a Known Amount of Dioxygen.[a]

Amount of O_2 (equiv)	Azobenzene (equiv)	DPH (equiv)
1	1.8	8.2
1	2.0	8.0
1	2.1	7.9
Average	2.0	8.0
2	4.1	5.9
2	3.9	6.1
2	3.9	6.1
Average	4.0	6.0
3	5.4	4.6
3	6.2	3.8
3	6.0	4.0
Average	5.9	4.1
4	7.8	2.2
4	8.0	2.0
4	8.4	1.6
Average	8.1	1.9
5	9.5	0.5
5	10.	0.03
5	9.8	0.2
Average	9.8	0.2

[a] Data in this table were used to generated Table 3.

Table S2. Relative Amounts of Water and Azobenzene Produced from Reactions of $[Mn^{II}H_2bupa]^-$ with DPH and Excess Dioxygen as Determined by ^1H NMR Spectroscopy.

Run	Relative Amt. DMSO	Relative Mole Ratio of H_2O[b]	Relative Mole Ratio of Azobenzene	Relative Mole Ratio of DPH	Relative Percent Yield
1[a]	1	0.41			
1	1	3.96 (3.55)	3.82	0.12	AB: 97% H_2O: 93%
2[a]	1	0.13			
2	1	10.62 (10.49)	10.97	0.18	AB: 98% H_2O: 95%
3[a]	1	0.06			
3	1	3.86 (3.80)	4.09	0.22	AB: 95% H_2O: 93%

[a] relative amount of water in DMSO-d_6; [b] values in parentheses are corrected for residual water in the DMSO-d_6 solvent and arise from integration of NMR resonances.

Table S3. Relative Amounts of Water Produced from Reactions of $[Mn^{II}H_2bupa]^-$ with DPH and Excess Dioxygen as Determined by Karl Fischer Titrations.

Run	Amount $[MnH_2bupa]$ (g)	Amt. DPH (g)	Theor. Amt. of H_2O (ppm)	Mass of Sample Used (g)	Experimental Determined H_2O (µg / ppm)	Mass of Background Sample (g)	Amount of Water In Backgrd. (µg/ppm)	Percentage of H_2O Produced
1	0.011g	0.069	2800	0.3001	897 /3000	0.2995	128 /430	93%
2	0.014	0.088	3100	0.3589	1210/ 3360	0.3700	55 / 150	105%

Table S4. Relative Amounts of Water Produced from Reactions of $[Mn^{II}H_2bupa]^-$ with Hydrazine and Excess Dioxygen as Determined by ^1H NMR Spectroscopy.

Run	Concentration of Toluene	Relative Amt. Toluene	Relative Mole Ratio of H_2O[b]	Equiv. of H_2O[c]	Equiv. of Hydrazine Used[c]	Relative Percent Yield of H_2O
1[a]		1	1.21			
1	0.160 M	1	3.14 (1.94)	17	8.79	97%
2[a]		1	10.86			
2	1.46 M	1	12.89 (2.03)	15.24	8.18	93%
3[a]		1	6.82			
3	0.155 M	1	8.62 (1.80)	13.81	7.62	91%

[a] relative amount of water in DMSO-d_6; [b] values in parentheses are corrected for residual water in the DMSO-d_6 solvent; [c] the amount of $[Mn(H_2bupa)]$- was set to one equivalent.

Table S5. Crystallographic Data for K[**1**]•0.5DMA.

Salt	K[**1**]•0.5DMA
Molecular formula	$C_{27}H_{47.5}KMnN_{7.5}O_{4.5}$
Formula weight (g/mol)	643.257
T (K)	150(2)
Space group	$P\bar{1}$
a (Å)	15.687(4)
b (Å)	20.310(5)
c (Å)	25.983(7)
α (deg)	95.152(4)
β (deg)	92.776(4)
γ (deg)	106.600(4)
Z	8
V (Å^3)	7877(3)
δ_{calcd} (Mg/m^3)	1.083
R[a]	0.0920
R_w[b]	0.2587
GOF[c]	1.002

[a] $R = [\Sigma|\Delta F|\Sigma|F_o|]$. [b] $R_w = \{\Sigma[\omega(F_o^2 - F_c^2)^2]/\Sigma[\omega(F_o^2)^2]\}^{1/2}$.
[c] Goodness of fit on F^2.

Table S6. N—C bond distances of the protonated and deprotonated forms of the 2-carboxyamidopyridyl unit.

Complex	Protonation State	N—C bond distance (Å)
1	-	1.338(7)
$[Mn^{II}H_2bupa]^-$	deprotonated	1.305(5)
$[Fe^{II}H_2bupa]^-$[a]	deprotonated	1.308(5)
$[Mn^{II}Hbpaa]$[b,c]	deprotonated	1.306(2)
	protonated	1.368(2)
$[Fe^{II}Hbpaa]$[d]	deprotonated	1.307(2)
	protonated	1.370(2)
H_5bupa[d]	protonated	1.366(6)
H_3bpaa[d]	protonated	1.371(2)
	protonated	1.372(2)

[a]reference 1; [b]reference 2; [c]$[Hbpaa]^{2-}$, *N*-[bis(6-pivalamido-2-pyridylmethyl)](*N'*-4-fluorophenylcarbamoylmethyl)aminato; [d]reference 3.

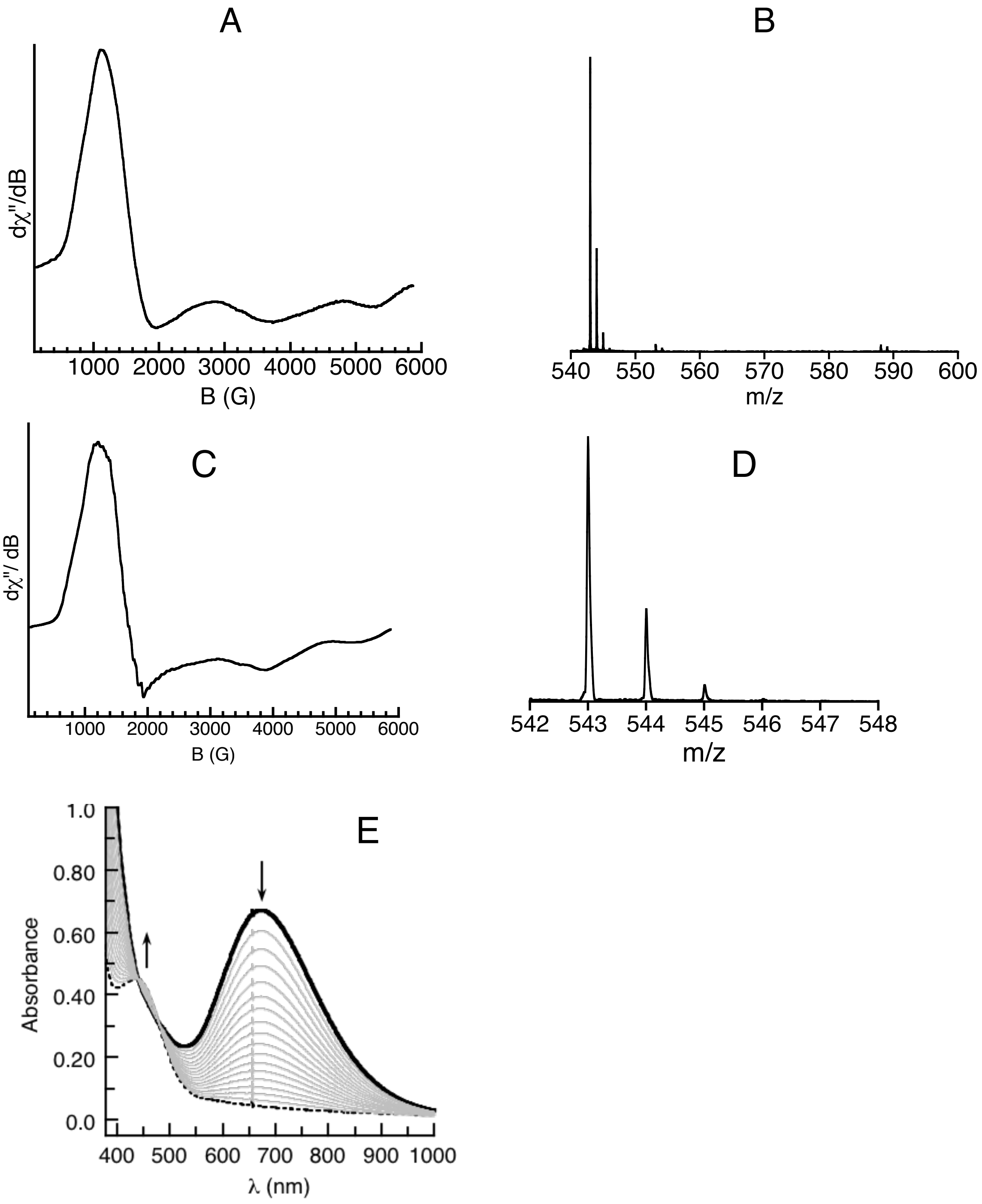

Figure S1. Perpendicular-mode X-band EPR spectrum (**A**) and ESI mass spectrum (**B**) after treating **1** with DPH, the corresponding spectra (**C,D**) of independently prepared $[\mathrm{Mn^{II}H_2bupa}]^-$, and optical spectra showing the conversion of **1** (—) to $[\mathrm{Mn^{II}H_2bupa}]^-$ and azobenzene (---). The peak at λ_{max} ~ 440 nm is from azobenzene.

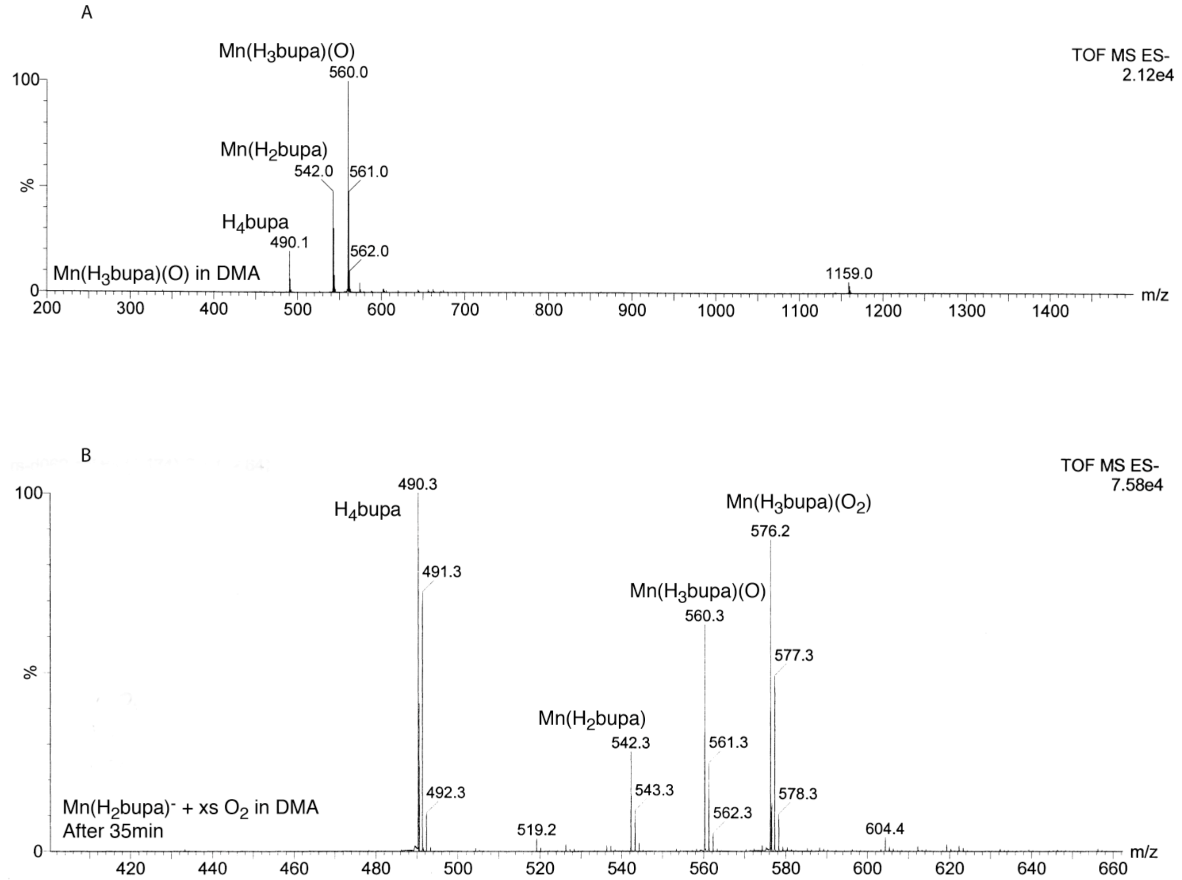

Figure S2. ESI-MS spectra (expanded-scale from those in Figure 2) for recrystallized **1** (**A**) and one for the reaction of $[Mn^{II}H_2bupa]^-$ with dioxygen after ~40 min, showing the presence of both $[Mn^{III}H_3bupa(O_2)]^-$ to **1** (**B**). The small peak at m/z = 1159 was modeled as a $K\{[Mn^{III}H_3bupa(O_2)]^-\}_2$ aggregate.

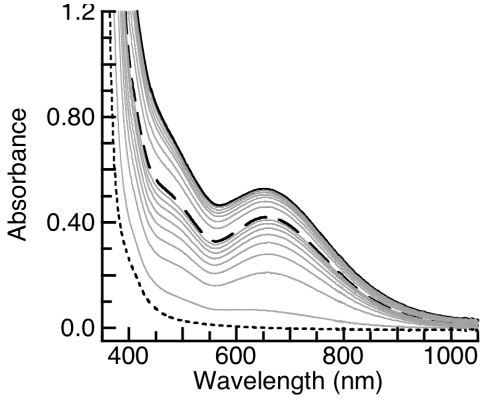

Figure S3. Electronic absorbance spectra illustrating the conversion of $[Mn^{II}H_2bupa]^-$ to $[Mn^{III}H_3bupa(O_2)]^-$ (- - -), and $[Mn^{III}H_3bupa(O_2)]^-$ to **1** (—) measured in DMA at room temperature. Spectra for the formation of $[Mn^{III}H_3bupa(O_2)]^-$ were recorded every 10 min and those for the conversion of $[Mn^{III}H_3bupa(O_2)]^-$ to **1** were collected every 30 min (total time was 5 h). The concentration of $[Mn^{II}H_2bupa]^-$ was 2.1 mM.

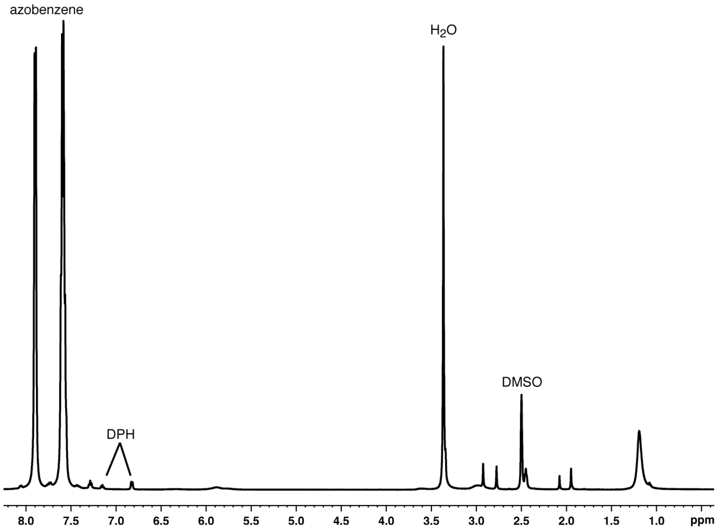

Figure S4. Example of an ^{1}H NMR spectrum for the conversion of DPH to azobenzene with [Mn^{II}H$_2$bupa]$^-$ and O$_2$.